Controlled overturning of unanchored rigid bodies

Rubén Boroschek[1,*,†,‡] and Antonio Iruretagoyena[2,§]

[1]*Civil Engineering Department, University of Chile, Blanco Encalada 2002, Santiago, Chile*
[2]*Civil Engineering Department, University of Chile, Chile*

SUMMARY

Typical small hospital and laboratory equipment and general supplies cannot be anchored to resist earthquake motions. In order to protect these non-structural components, a common procedure is to provide barriers to restrain overturning of objects on shelves and other furniture. In many cases this option is not available, especially for hospital equipment, because of other functional requirements. This work presents an alternative approach. The method proposed here does not avoid overturning, but controls the direction of overturning by providing an inclination to the support base so that the overturning occurs in a preferential direction towards a safe area. For example, objects on shelves, could overturn towards the inside or a wall, and equipment on tables could overturn away from the edge. In both cases this would not only reduce the damage to the particular items, but reduce the amount of debris on the floor.

In order to determine the proper inclination of the base, specific rigid bodies are analytically evaluated for bi-directional excitation obtained from 314 earthquake records, in approximately 7500 cases. For each case, several inclination angles are evaluated. Finally, a parametric curve is adjusted to the data, given a relation between angle of inclination and percentage of controlled overturning cases. In all cases a 7° angle gives more than 98% confidence of controlled overturning. The design expressions were later compared with experimental results obtained on a six-degree-of-freedom shake table; confirming the analytical expressions.

KEY WORDS: rocking; rigid block; unanchored block; rigid body; overturning

INTRODUCTION

By seismic excitation, an unanchored object may enter a rocking state which could cause it to finally overturn. If we think of all the unanchored objects that rest on shelves, racks and tabletops, and consider the eventual possibility of them overturning or collapsing, then we would understand the importance of developing a system that can increase our security by preventing them from overturning in an unsafe way.

*Correspondence to: Rubén Boroschek, Civil Engineering Department, University of Chile, Blanco Encalada 2002, Santiago, Chile.
†E-mail: rborosch@ing.uchile.cl
‡Assistant Professor.
§Engineering Student.

The method suggested here, would not prevent objects from overturning, but will force them to overturn in a desired direction. This means we can make objects overturn towards a safe zone where no damage will be done. In order to force this effect we induce a small slope to the plane where the objects lay, in the direction that we want them to overturn.

PREVIOUS RESEARCH

According to Ishiyama [1], the dynamic behaviour of a rigid block over an oscillating surface has been the subject of investigation since 1881 with the works of Milne and Perry for horizontal acceleration and in 1924 with Mononobe including vertical influence. Housner [2] established overturning criteria for tall, slender structures subject to horizontal acceleration, motivated by the observed behaviour in water towers during the Chilean earthquake of 1960. He proposed an energy balance equation to determine the pseudo-velocity S_v needed to obtain a 50% of overturning rate.

Yim *et al.* [3] investigated the rocking response for an unanchored rigid body that cannot slide. They use horizontal and vertical accelerations to determine the effects that the properties of the acceleration have over the behaviour of the body. They determined that the rocking state of a rigid body is very sensitive to the geometric properties of the body as to the properties of the acceleration applied.

Ishiyama [4], classified and studied the different dynamic stages that describe the behaviour of the rigid body under seismic excitation: rest, slide, jump, rotate, slide and rotate, and impact. He determined the movement equations for each case and the criteria to establish the boundaries between them. Uematsu *et al.* [5] present factors that can be included to improve the similarities between the analytic and experimental response. Shenton [6], studied in depth some of the boundary criteria of the different dynamic stages.

Recent works of Fierro and Perry [7], Kaneko and Hayashi [8] and Boroschek and Romo [9] are oriented to obtaining design criteria in order to solve the overturning of unanchored rigid bodies under seismic excitation. In the works of Fierro and Perry [7], the influence of the geometric properties of the body and input displacement on its overturning are presented. Boroschek and Romo [9], included asymmetric bodies and reestablished the overturning criteria for these cases. On the other hand, Kaneko and Hayashi [8] studied the overturning behaviour of different bodies and proposed an equation to obtain the overturning ratio for a specific body, which depends on the geometric properties of the body and the properties of the input excitation.

All the works previously mentioned studied the response of unanchored objects on a horizontal plane, although there is one work by Plaut *et al.* [10] that included inclined planes. The work described the fractal behaviour that can be found in the overturning of a body, subject to its chaotic response.

PHYSICAL THEORY

By developing the static equilibrium equations of an unanchored object placed on an inclined plane, we can determinate the acceleration needed to initiate a rotation over the body.

We define h and b as the geometric dimensions of the body, where β is the plane inclination and a_{yg}, a_{xg} are the corresponding floor accelerations, Figure 1. The equation for the horizontal

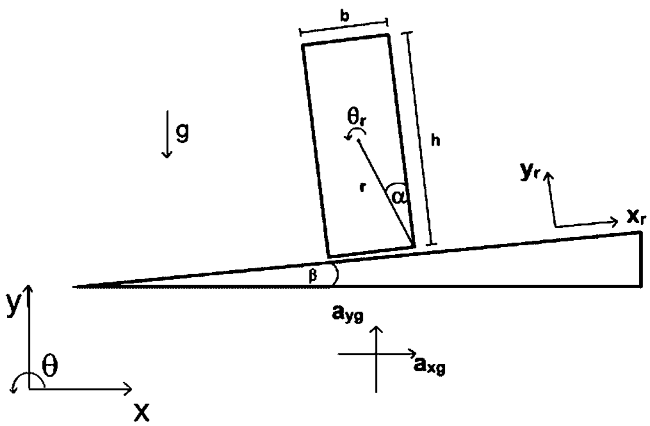

Figure 1. Diagram of a rigid body on an inclined plane, subject to vertical and horizontal accelerations.

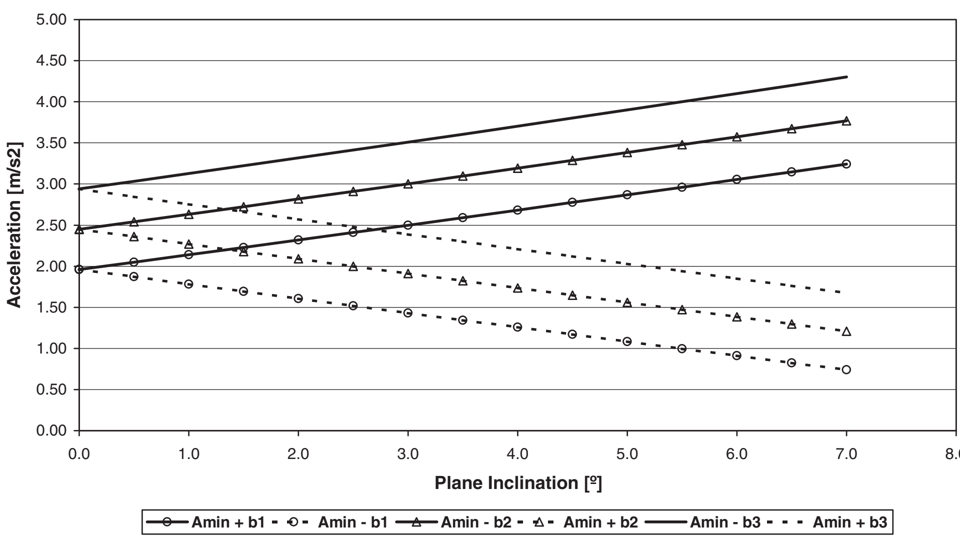

Figure 2. Minimum acceleration needed to initiate rotation of the body in the same and opposite direction of the plane inclination.

acceleration needed to initiate rocking may be written as

$$a_{xg} = \frac{(a_{yg} + g)\left(\dfrac{b}{h} - \tan\beta\right)}{\left(1 + \dfrac{b}{h}\tan\beta\right)} \tag{1}$$

Figure 2 shows the values for the acceleration of three different bodies ($b1[b/h = 0.2]$, $b2[b/h = 0.25]$, $b3[b/h = 0.3]$). It shows the minimum acceleration needed to initiate rotation in the opposite direction of the plane, '$A_{\min^-}$', and the minimum acceleration needed to initiate rotation in the same direction of the plane, '$A_{\min^+}$'. As we can see in this figure, for greater slopes, a greater acceleration is needed to rotate the body in the opposite direction of the slope, while for the same direction, a lower acceleration is needed. From this, we can propose a method to control the overturning direction of a body subject to seismic acceleration by applying a specific inclination to its supporting plane. We must also consider that by doing this we also increase the probability of overturning.

ROCKING CONTROL

To describe the dynamic behaviour of an unanchored body we will use two analytic methods: the first one consists of the solution of the specific rocking equation and the other consists of the solution of a general equation for the different dynamic stages of the body.

Rocking equation

The specific equation that describes the rocking behaviour of an unanchored object on a horizontal plane has been previously studied and it is well discussed in the works of Yim *et al.* [3]. We have modified this equation in order to extend its application to non-horizontal planes, resulting in:

$$\ddot{\theta}_r = -p^2 \left[\sin(\alpha\,\mathrm{sign}(\theta_r) - \theta_r + \beta) \cdot \left(1 + \frac{a_{yg}}{g}\right) + \frac{a_{xg}}{g} \cos(\alpha\,\mathrm{sign}(\theta_r) - \theta_r + \beta) \right] \qquad (2)$$

where $p = \sqrt{3g/4r}$; a_{yg} is the vertical acceleration; β the plane inclination; a_{xg} the horizontal acceleration; $\alpha = \tan^{-1}(b/h)$; $r^2 = (b^2 + h^2)/4$; $\mathrm{sign}(\theta_r) = +1$ or -1 depending on the sign of the angle θ_r. $\mathrm{sign}(0) = +1$; β, b, h are as shown in Figure 1; X_r, Y_r, θ_r correspond to the coordinate system associated to the inclined plane as shown in Figure 1.

General equation

For a second method we have solved the equations of the different dynamic stages of a body subject to ground acceleration presented by Ishiyama [4], which result in a faster method for resolving the dynamic response of the unanchored object.

The different stages proposed are: rest, slide, rotation, jump, rotation with sliding, and impact. These equations have been modified in order to use them on an inclined plane and are shown as follows:

Rest:

$$R_y = (a_{yg} + g)\cos\beta + a_{xg}\sin\beta > 0 \qquad (3)$$

$$R_x = a_{xg}\cos\beta + (a_{yg} + g)\sin\beta \qquad (4)$$

where R_y and R_x are the reactions by unit of mass of the body over the foundation.
Pure slide:

$$\ddot{x}_r = -(a_{yg} + g)(\mathrm{sign}(\dot{x}_r)\cos\beta\mu_k + \sin\beta) - a_{xg}(\cos\beta + \mathrm{sign}(\dot{x}_r)\sin\beta\mu_k) \qquad (5)$$

Pure rotation:

$$\ddot{\theta}_r = \frac{r}{i_g^2 + r^2}\begin{bmatrix}\cos(\alpha - |\theta_r|)[(a_{yg} + g)\sin\beta + a_{xg}\cos\beta] - \\ s_1 \sin(\alpha - |\theta_r|)[(a_{yg} + g)\cos\beta + a_{xg}\sin\beta]\end{bmatrix}$$

$$s_1 = \mathrm{sign}(\theta_r), \qquad \theta_r \neq 0 \tag{6}$$

$$s_1 = \mathrm{sign}(\dot{\theta}_r), \qquad \theta_r = 0 \wedge \dot{\theta}_r \neq 0$$

$$s_1 = \mathrm{sign}[a_{xg}\cos\beta + (a_{yg} + g)\sin\beta], \qquad \theta_r = 0 \wedge \dot{\theta}_r = 0$$

Pure jump:

$$\ddot{x}_r = -a_{xg}\cos\beta - (a_{yg} + g)\sin\beta \tag{7}$$

$$\ddot{y}_r = -(a_{yg} + g)\cos\beta - a_{xg}\sin\beta \tag{8}$$

Rotation with displacement:

$$\ddot{\theta}_r = \frac{s'' r[rc\dot{\theta}_r^2 - (a_{yg} + g)\cos\beta - a_{xg}\sin\beta][s + s's''\mu_k c]}{r^2 s[s + s's''\mu_k c] + i_g^2} \tag{9}$$

$$\ddot{x}_r = s'\mu_k[r\dot{\theta}_r^2 c - s'' r\ddot{\theta}_r s - (a_{yg} + g)\cos\beta - a_{xg}\sin\beta] - a_{xg}\cos\beta - (a_{yg} + g)\sin\beta \tag{10}$$

with

$$s' = \mathrm{sign}(\dot{x}_{ro}) \quad \text{if } \dot{x}_{ro} \neq 0$$

$$s' = \mathrm{sign}(-a_{xg}\cos\beta - (a_{yg} + g)\sin\beta) \quad \text{if } \dot{x}_{ro} = 0 \text{ and } a_{xg} \neq 0$$

$$s' = \mathrm{sign}(-\theta_r(\alpha - |\theta_r| - \mathrm{sign}(\theta_r)\beta)) \quad \text{if } \dot{x}_{ro} = 0 \text{ and } a_{xg} = 0$$

$$s'' = \mathrm{sign}(\theta_r) \quad \text{if } \theta_r \neq 0$$

$$s'' = \mathrm{sign}(\dot{\theta}_r) \quad \text{if } \theta_r = 0 \text{ and } \dot{\theta}_r \neq 0$$

$$s'' = \mathrm{sign}(a_{xg}\cos\beta + (a_{yg} + g)\sin\beta) \quad \text{if } \theta_r = 0 \text{ and } \dot{\theta}_r = 0$$

$$c = \cos(\alpha - |\theta_r|)$$

$$s = \sin(\alpha - |\theta_r|)$$

ANALYTICAL RESULTS

All the analytic study was developed considering a plastic impact, i.e. using a coefficient of restitution equal to zero. The equations do not present this term because it only defines

Table I. Dimensions of the 12 bodies used in the analytical study.

Body	1	2	3	4	5	6	7	8	9	10	11	12
Base (m)	0.04	0.05	0.06	0.10	0.13	0.15	0.18	0.20	0.25	0.30	0.30	0.38
Height (m)	0.20	0.20	0.20	0.50	0.50	0.50	0.50	1.00	1.00	1.00	1.50	1.50
b/h (dimensionless)	0.20	0.25	0.30	0.20	0.26	0.30	0.36	0.20	0.25	0.30	0.20	0.25
r (m)	0.10	0.10	0.10	0.25	0.26	0.26	0.27	0.51	0.52	0.52	0.76	0.77
α (rad)	0.20	0.24	0.29	0.20	0.25	0.29	0.35	0.20	0.24	0.29	0.20	0.25
# Records (dimensionless)	258	196	158	258	188	158	116	258	196	158	258	196

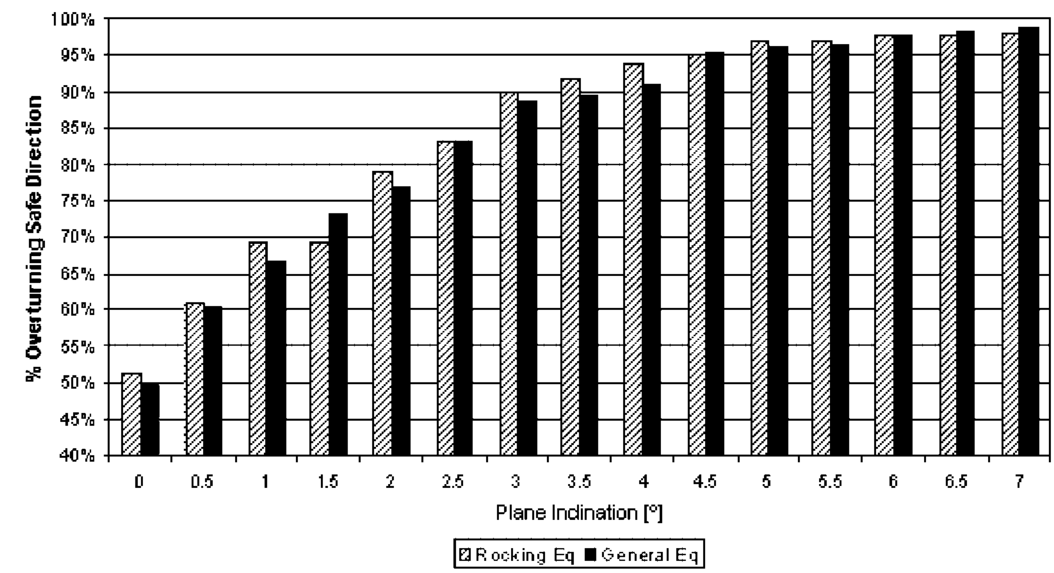

Angle[°]	0	0,5	1	1,5	2	2,5	3	3,5	4	4,5	5	5,5	6	6,5	7
Rocking Eq	51%	61%	69%	69%	79%	83%	90%	92%	94%	95%	97%	97%	98%	98%	98%
Gral Eq	50%	60%	67%	73%	77%	83%	89%	89%	91%	95%	96%	96%	98%	98%	99%
Overturn #	170	172	175	187	192	205	213	223	228	233	238	243	246	248	251

Figure 3. Analytical results corresponding to body #1 (b:0.04, h:0.2).

borders conditions between motion stages. In the case of the general equation we used a high frictional coefficient in order to avoid the body from sliding, which represent a more critical case to study the rocking behaviour.

To build the analytical results, we studied the response of 12 bodies (Table I), subject to 314 earthquake records obtained from the following earthquakes: Taiwan 1999, Kern County 1952, Northridge 1994, Chile 1985, Kobe 1995, Kocaeli 1999, Landers 1992, Loma Prieta 1989, Imperial Valley 1979, Morgan Hill 1984, San Fernando 1971, Borego Mountain 1968, Palm Springs 1986, Sierra Madre 1991 and Whittier 1987. The records were entered with their horizontal and vertical components and the horizontal direction was analysed for both signs.

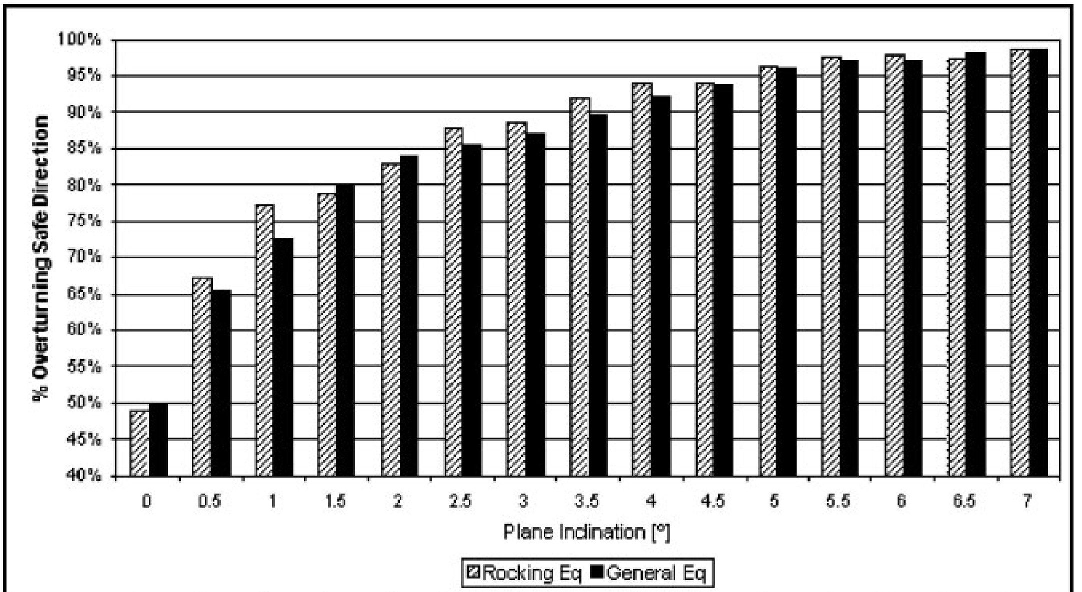

Angle [°]	0	0,5	1	1,5	2	2,5	3	3,5	4	4,5	5	5,5	6	6,5	7
Rocking Eq	49%	67%	77%	79%	83%	88%	88%	92%	94%	94%	96%	98%	98%	97%	99%
Gral Eq	50%	65%	73%	80%	84%	86%	87%	90%	92%	94%	96%	97%	97%	98%	98%
Overturn #	107	113	113	121	126	140	151	161	173	177	188	195	206	214	220

Figure 4. Analytical results corresponding to body #4 (b:0.10, h:0.5).

The number of records that generated overturning were counted for each body, classifying them according to the overturning direction. By this procedure we obtained an overturning rate in the desired direction for each body along with its respective plane inclination. In order to decrease the processing time for each analysis, only the records that satisfy the minimum acceleration criteria (1) for the horizontal plane were used. The corresponding results are presented in Figures 3–6.

As seen in these figures, the results obtained by both methods are very similar. In general we can observe that the difference between them is smaller than 4% for all the experiments. The use of one or the other method depends on utilization advantages, like simplicity or processing speed rather than for the results. Figure 6 shows the average results for all the bodies using both methods. In this figure we can distinguish a characteristic behaviour of the curves for all the bodies. They have a predictable behaviour that can be represented by an analytic expression. The behaviour of the curves is very similar for the different bodies. If we obtain an average curve for all the bodies and compare it with the results we found differences lower than 15% for the worst case. Because of this we propose to model the percentage of controlled overturning rate with two different analytic expressions: the first one corresponds to the average behaviour for all the bodies (general controlled overturning rate, GCOR), and the second includes the dimensions of the body as one of its variables (specific controlled overturning rate, SCOR).

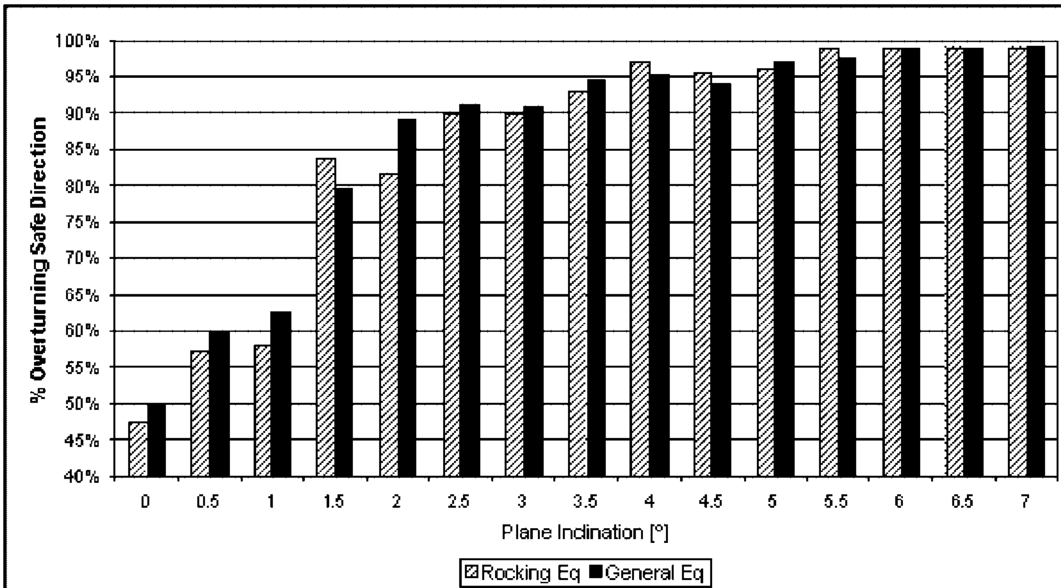

Angle [°]	0	0,5	1	1,5	2	2,5	3	3,5	4	4,5	5	5,5	6	6,5	7
Rocking Eq	47%	57%	58%	84%	82%	90%	90%	93%	97%	95%	96%	99%	99%	99%	99%
Gral Eq	50%	60%	63%	80%	89%	91%	91%	94%	95%	94%	97%	98%	99%	99%	99%
Overturn #	36	36	36	43	47	50	55	56	64	70	76	85	91	102	112

Figure 5. Analytical results corresponding to body #12 (b:0.38, h:1.5).

The values for the GCOR can be seen in Figure 6. The expression is the following:

$$\mathrm{GCOR} = \tanh\left(\frac{\beta}{c1}\right) c2 + 0.5 \tag{11}$$

With $c1 = 0.048$, $c2 = 0.48$, and β being the plane inclination (rad).

The results obtained using this expression are shown in Table II. This analytic expression corresponds to the average behaviour for any body, independently of its dimensions. Figure 7 shows the values of this equation in comparison with the average of the analytic results. The percentage of error displayed in Figure 7 is obtained using the following expression:

$$\sqrt{\frac{\sum (X_i - X_f)^2}{\sum X_f^2}} \tag{12}$$

where X_i refers to the analytical results and X_f to the values obtained by the GCOR expression. Figure 7 shows that the proposed curve has a conservative behaviour for small inclinations. In addition, from Figure 6 we can say that generally the values obtained by this equation result in a conservative response for bigger bodies.

The second equation proposed corresponds to a more specific expression in which the dimensions of the body are considered, defined as SCOR. In this way we obtained a more representative response for each particular body, although that this expression is applicable

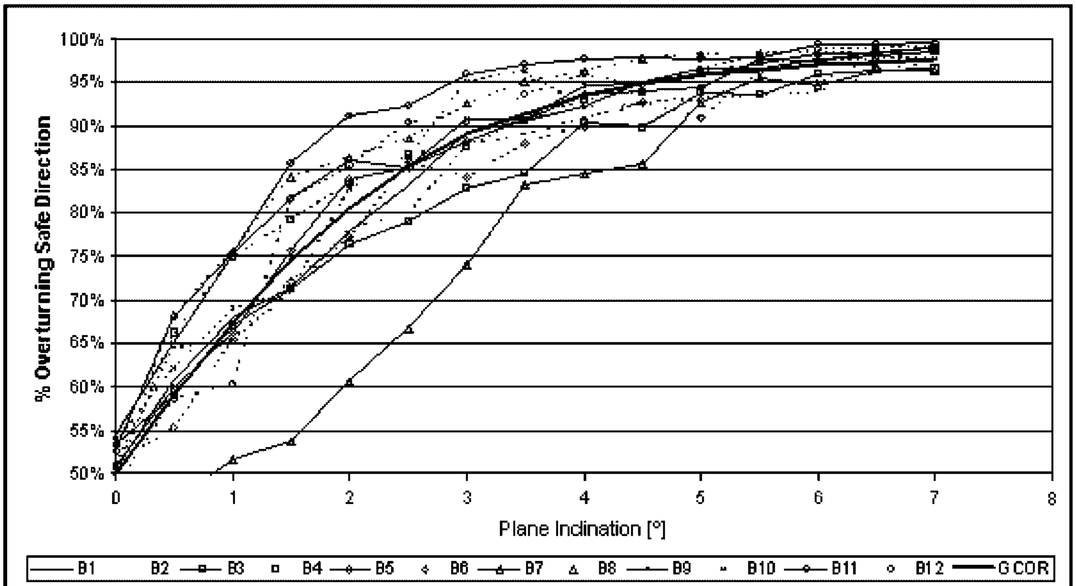

Body		1	2	3	4	5	6	7	8	9	10	11	12
Base	[m]	0.04	0.05	0.06	0.10	0.13	0.15	0.18	0.20	0.25	0.30	0.30	0.38
Height	[m]	0.20	0.20	0.20	0.50	0.50	0.50	0.50	1.00	1.00	1.00	1.50	1.50
b/h	[ ]	0.20	0.25	0.30	0.20	0.26	0.30	0.36	0.20	0.25	0.30	0.20	0.25
r	[m]	0.10	0.10	0.10	0.25	0.26	0.26	0.27	0.51	0.52	0.52	0.76	0.77
α	[rad]	0.20	0.24	0.29	0.20	0.25	0.29	0.35	0.20	0.24	0.29	0.20	0.25

Figure 6. Average results for all the bodies using both analytical methods, the rocking equation and the general equation.

Table II. Controlled overturning rate obtained by using the GCOR equation for inclinations from 0 to 7°.

Angle (°)	0	0.5	1	1.5	2	2.5	3	3.5	4	4.5	5	5.5	6	6.5	7
%	50	59	67	75	81	85	89	92	94	95	96	97	97	97	98

only when the body dimensions are known. This equation is used for the design of a support base for a specific body; its expression is the following:

$$\mathrm{SCOR} = \tanh\left(\frac{\beta}{c1}\right) c2 + 0.5 \tag{13}$$

with $c1 = 0.1136(b/h) - 0.0283r + 0.0279$, $c2 = 0.48$, β the plane inclination (rad), b the width (m), h the height (m), $r = \sqrt{(b/2)^2 + (h/2)^2}$ (m).

In order to compare both expressions, we can observe in Figures 8 and 9 the values for these expressions for the different bodies and their respective analytic results.

Table III shows some error estimators used to compare both equations, where 'GCOR' refers to the average equation and 'SCOR' refers to the characteristic equation.

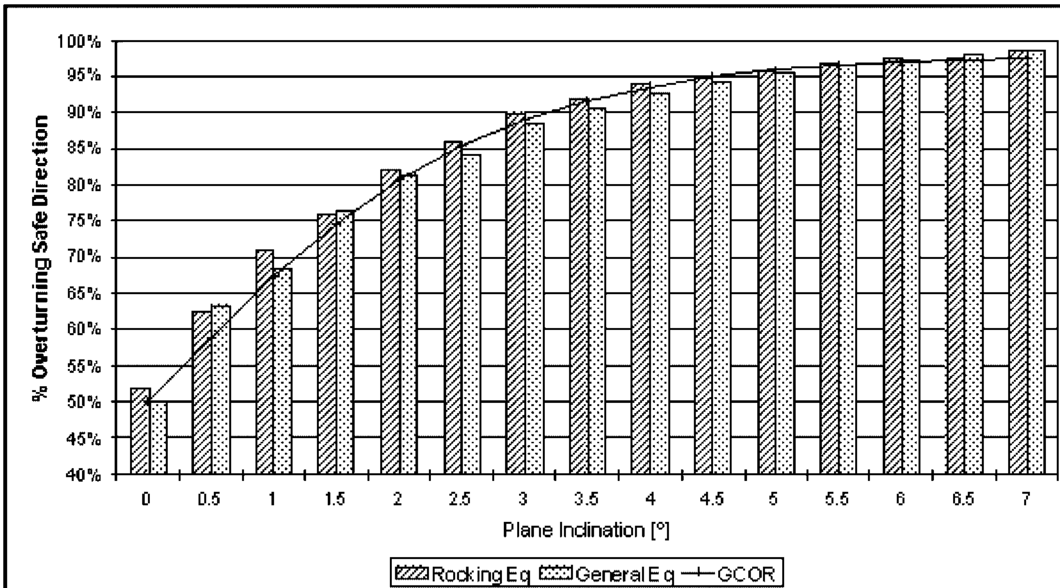

Angle	0	0.5	1	1.5	2	2.5	3	3.5	4	4.5	5	5.5	6	6.5	7	error %
General Eq	50%	63 %	68 %	77 %	81%	84%	88%	91 %	93 %	94%	95 %	97%	97 %	98 %	99 %	1.67%
Rocking Eq	52%	62 %	71 %	76 %	82%	86 %	90%	92 %	94 %	95 %	96 %	97%	97 %	98 %	98 %	1.74%
GCOR	50%	59 %	67 %	75 %	81%	85 %	89%	92 %	94 %	95 %	96 %	97%	97 %	97 %	98 %	

Figure 7. Comparison between the GCOR equation, and the average behaviour for all the bodies' dimensions obtained from the analytical study.

The improvement obtained by using the SCOR equation is better observed in Figure 9, where the particular cases can be seen. In general, the most significant improvements occur for the bigger bodies; also we can observe that for those bodies the equations have a conservative estimation.

In view of the fact that the difference between both equations is not relevant, the use of one or the other will depend solely on the final application.

Throughout the study we could observe that for a given aspect ratio, increasing the size of the body made it easier to control its direction of overturning. We can observe this phenomenon in Figure 10, where the response of different bodies with equal aspect ratio is shown.

EXPERIMENTAL RESULTS

In order to verify the results obtained from the analytical study, an experimental research was also performed. We studied the behaviour of seven bodies previously studied with the analytical method. The selection criterion was based on the aspect ratio of the bodies in order to ensure the study of relevant cases. The height of the bodies selected was limited to a maximum of 1 m to avoid test accidents due to the weight that these bodies represent. To

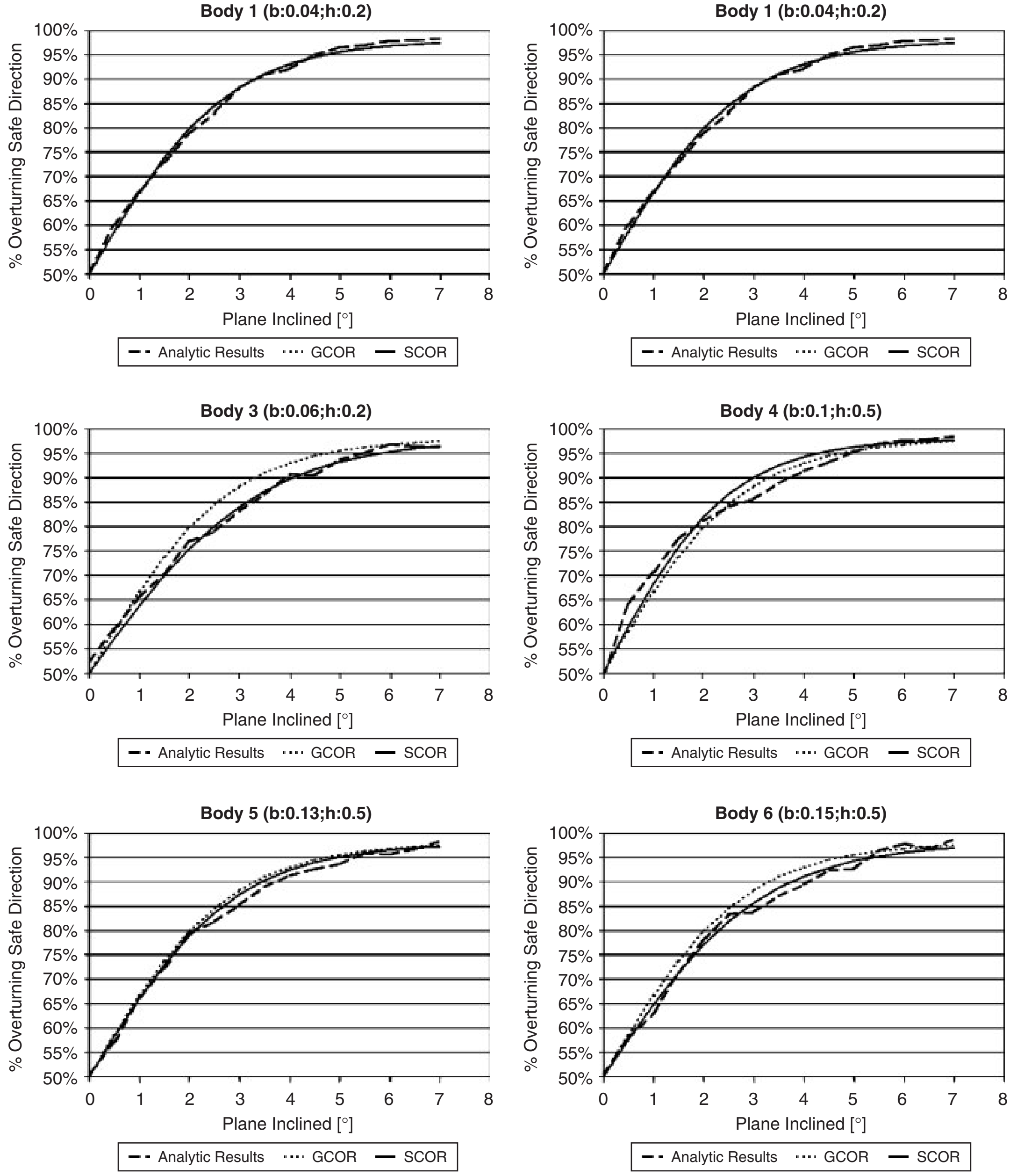

Figure 8. The results obtained from the analytical method, from the GCOR equation and from the SCOR equation for bodies 1–6 are shown.

simulate the seismic excitation in the base of the bodies, we used a shaking table with six degrees of freedom as shown in Figure 11. The table has a load capacity of 10 kN and its nominal dynamic limitations are shown in Table IV.

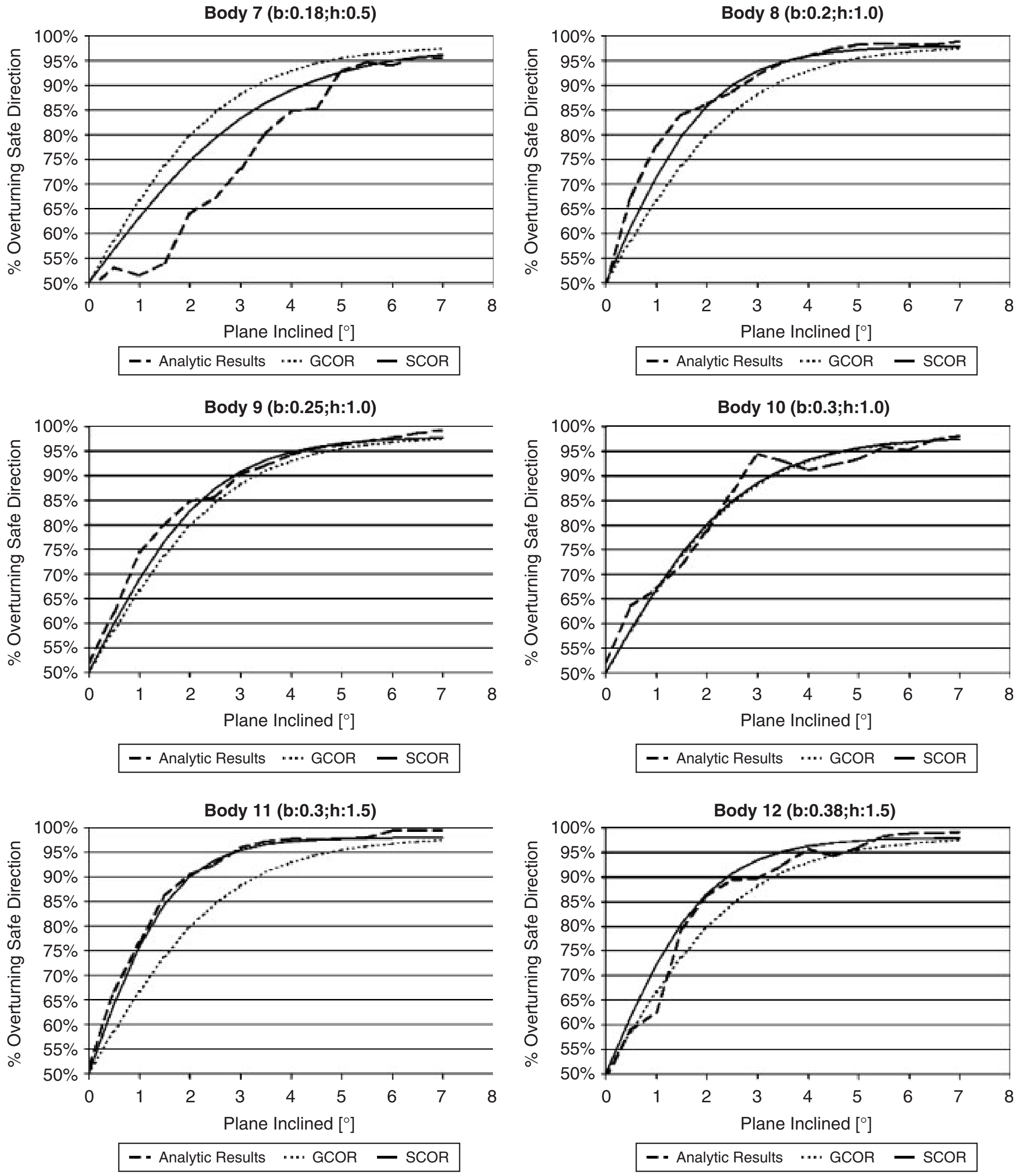

Figure 9. The results obtained from the analytical method, from the GCOR equation and from the SCOR equation for bodies 7–12 are shown.

Table III. Error estimators used to compare both equations proposed, the GCOR equation and the SCOR equation, using the analytical results as reference.

	Geometric properties					Max difference		Absolute area		Error	
Body	Base	Height	b/h	r	α	GCOR (%)	SCOR (%)	GCOR	SCOR	GCOR (%)	SCOR (%)
1	0.04	0.2	0.20	0.10	0.20	3	−2	5.01	5.21	1	1
2	0.05	0.2	0.25	0.10	0.24	9	10	15.57	8.22	3	2
3	0.06	0.2	0.30	0.10	0.29	−7	5	16.83	5.86	3	2
4	0.10	0.5	0.20	0.25	0.20	9	7	12.39	13.22	3	3
5	0.13	0.5	0.26	0.26	0.25	−3	−3	9.23	5.87	2	1
6	0.15	0.5	0.30	0.26	0.29	−5	−2	13.90	6.65	3	2
7	0.18	0.5	0.36	0.27	0.35	−37	−29	63.12	40.98	13	9
8	0.20	1.0	0.20	0.51	0.20	14	8	31.50	11.65	6	3
9	0.25	1.0	0.25	0.52	0.24	10	7	17.61	9.23	4	2
10	0.30	1.0	0.30	0.52	0.29	7	6	12.39	12.35	3	3
11	0.30	1.5	0.20	0.76	0.20	14	4	41.16	6.04	8	1
12	0.38	1.5	0.25	0.77	0.25	7	−16	15.13	14.91	4	3

Three column shows the different estimators used: *Max difference*, correspond to the maximum difference observed between each equation and the analytical results. *Absolute Area*, correspond to the absolute area between each equation and the analytical results. *Error*, correspond to the error between each equation and the analytical result using Equation (12).

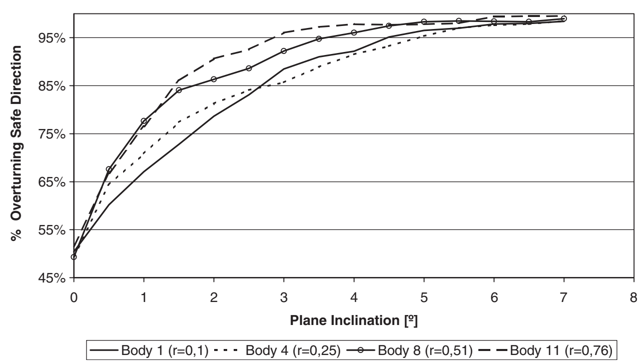

Figure 10. Results obtained for different bodies with the same aspect ratio ($h/b = 5$).

To build the bodies we used agglomerated wood in order to obtain a relatively homogeneous mass distribution, the respective sizes and positions of their centre of mass are shown in Table V. The depth of each body was as a minimum twice its width, in order to avoid a torsional motion. To keep the bodies from sliding, rough surfaces were used to generate a high static friction coefficient to ensure a rocking state of the body before sliding.

Figure 12 shows a picture of the bodies used along with the table assembly. The rectangular objects shown over the table correspond to shock absorbers, which were used to prevent the bodies from hitting the table.

Figure 11. General view of the shaking table. Test procedure.

Table IV. Shaking table motion nominal limits.

Axis	Displacement (m)	Velocity (m/s)	Acceleration (g)
Surge	± 0.25	± 0.5	± 0.6
Lateral	± 0.25	± 0.5	± 0.6
Heave	± 0.18	± 0.3	± 0.7

Table V. Dimensions of the seven bodies used in the shaking table study.

Body	Base (mm)	Height (mm)	Depth (mm)	Aspect ratio b/h (dimensionless)	Mass (kg)	Centre of gravity bcg (mm)	Centre of gravity hcg (mm)
1	99	493	201.2	0.20	5.22	51.5	243
2	130	500	305	0.26	13.11	65	254
3	152	500	301.5	0.30	15.31	76.5	251.5
4	39	200	81	0.20	0.36	19.5	100
5	49	200	109	0.25	0.56	25	100
6	200	998	410	0.20	54.96	100	495
7	248	995	490	0.25	65.14	124	499

The earthquake records used correspond to a selection of 25 records out of the total 314 used in the analytic research. The selection was based on those that resulted in a greater number of overturned objects, which in most cases were the ones with greater acceleration values. Unfortunately, some of these records surpass the physical limits of the shaking table, so it was necessary to scale some of them down. The records used and their corresponding scale factors are shown in Table VI.

Figure 12. Bodies used in the experimental analysis, along with the shaking table assembly.

Table VI. Earthquake records and scales.

Earthquake record	Scale
Kobe 1995, KJMA 090 - up	0.68
Northridge 1994, Sylmar 142 - up	0.57
Chi-Chi 1999 Taiwan, TCU068E - up	0.35
Imperial Valley 1979, Bonds Corner 140 - up	0.26
Imperial Valley 1979, Imperial Valley College, El Centro Array #7, CA S50W - up	0.49
Northridge 1994, Castaic - Old Ridge Route 090 - up	0.96
Loma Prieta 1989, Corralitos - Eureka Canyon Rd. 000 - up	0.91
Loma Prieta 1989, Corralitos - Eureka Canyon Rd. 090 - up	1
Northridge 1994, Castaic - Old Ridge Route 360 - up	0.92
Chile 1985, Llolleo 10 - up	0.67
Chile 1985, Melipilla EW - up	1
Imperial Valley 1979, James Rd., El Centro Array #5, CA S50W - up	0.53
Landers 1992, Lucerne 270 - up	0.58
Loma Prieta 1989, Gilroy #1 - Gavilan College, Water Tank 090 - up	1
Whittier 1987, Bell - Bulk Mail Facility 280 - up	1
Loma Prieta 1989, Gilroy #3 - Gilroy Sewage Plant 000 - up	1
Imperial Valley 1979, Anderson Rd., El Centro Array #4 S40E - up	1
Chile 1985, Llay-Llay N80W - up	1
Imperial Valley 1979, Cruickshank Rd., El Centro Array #8, CA S40E - up	0.95
Kocaeli 1999 Turkey, DZC 270	0.93
Chile 1985, Llay-Llay S10W - up	1
Imperial Valley 1979, Imperial Valley College, El Centro Array #7, CA S40E - up	1
Northridge 1994, Arleta - Nordhoff Ave Fire Station 090 - up	0.91
Loma Prieta 1989, Gilroy #2 - HWY 101/Bolsa Rd. Motel 000 - up	1
Loma Prieta 1989, Gilroy #2 - HWY 101/Bolsa Rd. Motel 090 - up	1

The inclination angles studied correspond to a range around the inclination angle that resulted from the analytical research, which ensure an overturning control of 95%. In general, this range corresponds to angles between 4 and 5.5°; we also studied the response for the horizontal plane to obtain a basic reference. The angles generated by the table were checked using topographic equipment. The basic output data obtained from this experimental study corresponds to the occurrence of overturning and its direction.

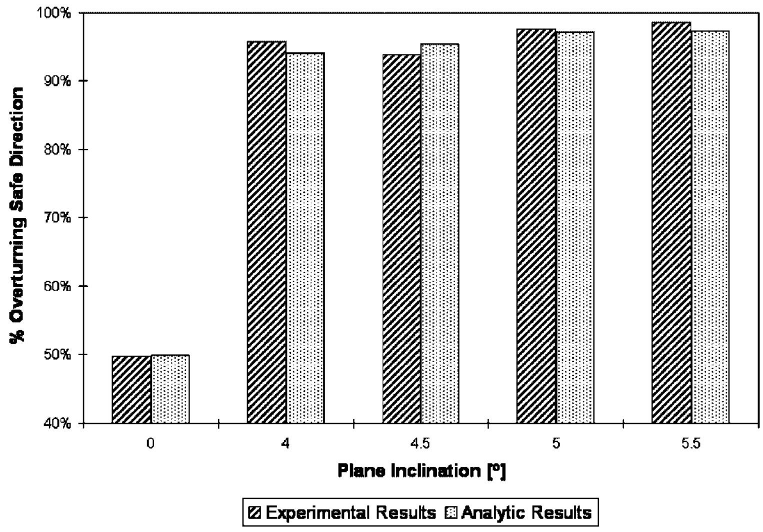

Figure 13. Comparison between the analytical and experimental research, using the average results for all the bodies studied.

In order to correlate the analytical and experimental results, we put accelerometers over the shaking table to record the actual table motion. With these values we developed the analytical results for the respective bodies and compared them with the experimental results. To compare the analytical and the experimental results, the overturning results obtained for each inclination angle and for each body for all the earthquake records were considered. In Figure 13, the experimental and the analytical results are compared for different angles and several bodies. In this figure the average overturning rate for each angle is presented. A maximum of 5% difference was found from the overturning rate for a given angle and specific body indicating the good agreement between analytical and experimental results.

CONCLUSIONS

The two analytical methods used in this work to describe the behaviour of an unanchored rigid body on a inclined plane show similar results and correlate well with the experimental results. Although they do not show significant difference in the results, each one has different programming advantages that must be considered.

In the results we can visualize the chaotic behaviour that represents the rocking motion of the bodies. In spite of this it was possible to control their overturning direction. In general we can observe that it was easier to control bigger bodies, as these needed smaller plane inclinations for the same overturning control rate.

It must be considered that all the results presented here are based on the fact that the bodies studied do, in fact, overturn. This means that the controlled overturning rate presented, indicates in which direction the body will overturn assuming that it will overturn. This important issue reduces the influence of the bodies' dimensions over the overturning results.

Two equations are determined to obtain the overturning rate direction, depending on their application. The first one corresponds to an equation independent of body dimensions.

$$\text{GCOR} = \tanh\left(\frac{\beta}{c1}\right)c2 + 0.5$$

With $c1 = 0.048$, $c_2 = 0.48$, and β being the plane inclination (rad).

The second equation corresponds to a more precise result in which the influences of body dimensions are considered.

$$\text{SCOR} = \tanh\left(\frac{\beta}{c1}\right)c2 + 0.5$$

With $c1 = 0.1136(b/h) - 0.0283r + 0.0279$, $c2 = 0.48$, b the width (m), β the plane inclination (rad), h the height (m), $r = \sqrt{(b/2)^2 + (h/2)^2}$ (m).

The estimation error observed using the first expression corresponds to an 8% in the worse case, in contrast with a 3% by using the second expression. By using these expressions we can estimate the angle of inclination needed for a plane to control the overturning direction of a rigid body, with a given probability factor associated.

Note that this study only considered overturning without sliding, and the records used correspond to ground-level acceleration.

By forcing items to overturn in a preferential direction we can improve the safety of many unanchored objects in laboratories, hospital and public places. We could reduce both damage to the items and collateral damage due to debris on floors or obstructed corridors by falling items.

REFERENCES

1. Ishiyama Y. Review and discussion on overturning of bodies by earthquake motions. *Research Paper No. 85*, Building Research Institute, 1980.
2. Housner G. The behavior of inverted pendulum structures during earthquakes. *Bulletin of Seismological Society of America* 1963; **53**(2):403–407.
3. Yim CS, Chopra AK, Penzien J. Rocking response of rigid blocks to earthquakes. *Report No. UCB/EERC-80/02*, Earthquake Engineering Research Center, University of California, Berkeley, CA, 1980.
4. Ishiyama Y. Motions of rigid bodies and criteria for overturning by earthquake excitations. *Earthquake Engineering and Structural Dynamics* 1982; **10**:635–650.
5. Uematsu T, Miyagi M, Ishiyama Y. Rocking motion and criteria for overturning of bodies on a floor—comparison between analysis and experiment. *Paper No. 2313*, 12th World Conference on Earthquake Engineering, 2000.
6. Shenton HW. Criteria for initiation of slide, rock, and slide rock rigid-body modes. *Journal of Engineering Mechanics* 1995; **122**(7):690–693.
7. Fierro E, Perry C. Overturning of rocking blocks. *Paper No. 1634*, 13th World Conference on Earthquake Engineering, Vancouver, Canada, 2004.
8. Kaneko M, Hayashi Y. A proposal for simple equations to express a relation between overturning ratios of rigid bodies and input excitations. *Paper No. 3299*, 13th World Conference on Earthquake Engineering, Vancouver, Canada, 2004.
9. Boroschek R, Romo D. Overturning criteria for non-anchored non-symmetric rigid bodies. *Paper No. 295*, 13th World Conference on Earthquake Engineering, Vancouver, Canada, 2004.
10. Plaut RH, Fielder WT, Virgin LN. Fractal behavior of an asymmetric rigid block overturning due to harmonic motion of a tilted foundation. *Chaos*, *Solitons and Fractals* 1995; **7**(2):177–196.